

Single top quarks at the Fermilab Tevatron

A. P. Heinson

Department of Physics, University of California, Riverside, California 92521

A. S. Belyaev and E. E. Boos

Institute of Nuclear Physics, Moscow State University, RU-119899 Moscow, Russia

(Received 19 December 1996)

We present a calculation of the single top quark cross section for proton-antiproton interactions with $\sqrt{s} = 1.8$ TeV at the Fermilab Tevatron collider. We examine the effects of the top quark mass, parton distribution functions, QCD scale, and collision energy, on each of the component production mechanisms, and study the kinematic distributions for standard model electroweak production. At the upgraded Tevatron with $\sqrt{s} = 2.0$ TeV and high luminosity, it will be possible to test the nature of the Wtb coupling using single top quark production. We estimate the sensitivity to measure the single top quark cross section, and thus to directly measure V_{tb} and the top quark partial width. We show what happens to the V_{tb} measurement when an anomalous ($V+A$) component is added to the Wtb coupling, and how the top quark polarization affects the kinematic distributions. [S0556-2821(97)05617-8]

PACS number(s): 14.70.Fm, 13.40.Em, 13.40.Gp

INTRODUCTION

Top quarks can be created via two independent production mechanisms in $p\bar{p}$ collisions. The primary mode, strong $t\bar{t}$ pair production from a $g\bar{t}t$ vertex, was used by the DØ and Collider Detector at Fermilab (CDF) Collaborations to establish the existence of the top quark in 1995 [1,2]. The second mode is the electroweak production of a single top quark or antiquark from a Wtb vertex. This mechanism provides a sensitive probe for several standard model parameters.

The experimental value of the top quark mass is 175 ± 6 GeV [3], which is in good agreement with the value of $177 \pm 7_{-19}^{+16}$ GeV derived from electroweak measurements at the CERN e^+e^- collider (LEP), SLAC Linear Collider, CERN Super Proton Synchrotron, Fermilab Tevatron, and neutrino scattering experiments [4]. Since the mass is of the order of the electroweak symmetry-breaking scale (vacuum expectation value = 246 GeV), it is a very promising place to look for deviations from the standard model [5].

The coupling between a W boson and top and bottom quarks has not yet been studied directly. Top quark pair production is not the best process for probing this Wtb coupling or the Cabibbo-Kobayashi-Maskawa (CKM) matrix element V_{tb} [6] since the top quarks are produced from a $g\bar{t}t$ vertex. Information about Wtb coupling from top quark decay is relatively inaccessible in $t\bar{t}$ pair production because the width of the decay into Wb is proportional to the branching fraction of $t \rightarrow Wb$, which is close to unity in the standard model [the top quark partial width $\Gamma(t \rightarrow Wb) \propto V_{tb}^2$, where $0.9989 \leq |V_{tb}| \leq 0.9993$ at the 90% confidence level [7]]. Single top quarks are produced at hadron colliders mainly from a Wtb vertex, and thereby provide a direct probe of the nature of the Wtb coupling and of V_{tb} .

In hadron collisions, there are several partonic processes which produce single top quarks in the final state. The W -gluon fusion mechanism $q'g \rightarrow tq\bar{b}$ has been studied in

Refs. [8–20]. The W^* s -channel process $q'\bar{q} \rightarrow t\bar{b}$ has been examined in Refs. [21–27] for the Tevatron. Use of single top quark production as a tool for studying the Wtb coupling has been discussed in a number of papers for hadron colliders, including the Tevatron [11,13,20,28–32]. Single top production has also been studied for e^+e^- colliders [28–30,33–43], and for $e\gamma$ interactions [44–46].

In this paper, we first present new results of consistent tree level cross section calculations for two and three vertex subprocesses of single top quark production in $p\bar{p}$ collisions at $\sqrt{s} = 1.8$ TeV. We have chosen to use this energy since it is where the Tevatron collider operated between 1992 and 1996, and this work is in support of a search of the data for single top production. We then prepare the ground for single top physics at future high luminosity Tevatron runs with $\sqrt{s} = 2.0$ TeV, by making new estimates of the sensitivity to measure the top quark partial width, Wtb coupling, and V_{tb} , including an anomalous ($V+A$) coupling. These studies are the first to be performed using complete tree level matrix element calculations for all possible processes, and do not use the effective W approximation method [8].

In Sec. I, we provide a comprehensive overview of the three separate single top processes at the Tevatron, and their subprocesses. We describe our computation techniques, and present and discuss the results of the calculations. We have studied the cross section as a function of top quark mass, parton distribution parametrization, choice of scale Q^2 , and collider energy, and we have evaluated lower and upper bounds on the single top quark cross section. In Sec. II of this paper, we investigate the kinematic distributions of single top quark events, showing the separate contributions from the principal production modes. In Sec. III, we look at the effects of a nonstandard coupling at the Wtb vertex, specifically the addition of an anomalous right-handed ($V+A$) contribution to the coupling. We estimate the sensitivity to determine V_{tb} by measuring the single top quark cross section at future Tevatron runs as a function of this possible

right-handed coupling strength, and show how the polarization of the system may be used to help distinguish different scenarios. We also use our estimate of the cross section precision to predict the error on the top quark partial width at the upgraded Tevatron. Finally, in the last section, we summarize our results and draw conclusions.

I. SINGLE TOP QUARK CROSS SECTION

A. Single top quark processes

Within the standard model, there are three separate processes at a proton-antiproton collider which result in a single top quark in the final state. The list below shows that these processes in turn consist of several subprocesses with two or three tree level vertices. The number of Feynman diagrams for each subprocess is shown. Some diagrams have been omitted from the total: (a) those with $t\bar{t}$ pair production from a $gt\bar{t}$ vertex and no electroweak vertex (not single top quark production); (b) those containing a photon, Z boson, or Higgs boson (their contribution to the total cross section is extremely small); and (c) diagrams with vertices containing off-diagonal CKM matrix elements. The notation used is that q is a light quark, and X represents any additional final state particles from the $p\bar{p}$ interaction.

- | | | |
|---|------------------------------------|---|
| (1) $p\bar{p} \rightarrow t\bar{b} + X$ | s -channel W^* boson | |
| 1.1 | $q'\bar{q}' \rightarrow t\bar{b}$ | 1 |
| 1.2 | $q'g \rightarrow t\bar{b}q$ | 2 |
| 1.3 | $q'\bar{q}' \rightarrow t\bar{b}g$ | 4 |
| (2) $p\bar{p} \rightarrow tq + X$ | t - or u -channel W boson | |
| 2.1 | $q'b \rightarrow tq$ | 1 |
| 2.2 | $q'g \rightarrow tq\bar{b}$ | 2 |
| 2.3 | $bg \rightarrow tq\bar{q}'$ | 2 |
| 2.4 | $q'b \rightarrow tqg$ | 4 |
| (3) $p\bar{p} \rightarrow tW^- + X$ | | |
| 3.1 | $bg \rightarrow tW$ | 2 |
| 3.2 | $q\bar{q}' \rightarrow tW\bar{b}$ | 2 |
| 3.3 | $gg \rightarrow tW\bar{b}$ | 5 |
| 3.4 | $b\bar{b} \rightarrow tW\bar{b}$ | 5 |
| 3.5 | $qb \rightarrow tWq$ | 3 |
| 3.6 | $bg \rightarrow tWg$ | 8 |

It should be noted that there is some variation in the literature over the use of the term “ W -gluon fusion.” In some papers it refers only to subprocess 2.2 $q'g \rightarrow tq\bar{b}$, in others to subprocesses 2.1 $q'b \rightarrow tq$ and 2.2 $q'g \rightarrow tq\bar{b}$ combined. Only one paper [17] includes all four subprocesses 2.1–2.4 in the calculations, and the authors use the term “ W -gluon fusion” to refer only to subprocess 2.2. In this paper, we will also use the term to mean only subprocess 2.2.

The two subprocesses 1.2 and 2.2 (both $q'g \rightarrow tq\bar{b}$), although superficially similar, each contain two different Feynman diagrams which are gauge invariant in separate pairs and do not need to be calculated together as a group of four diagrams. One might be tempted to consider the four dia-

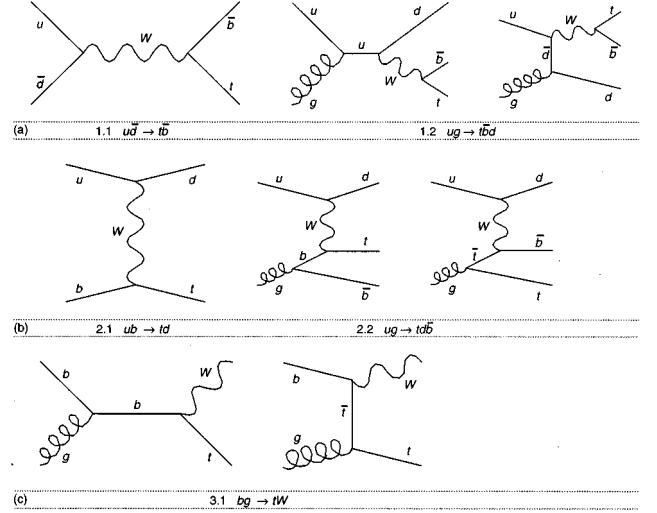


FIG. 1. Representative Feynman diagrams for the three single top quark production processes at the Fermilab Tevatron: (a) the W^* s -channel process $p\bar{p} \rightarrow t\bar{b} + X$; (b) the W t - and u -channel process $p\bar{p} \rightarrow tq + X$, including subprocess 2.2, W -gluon fusion; and (c) $p\bar{p} \rightarrow tW^- + X$.

grams as an independent set instead of as separate higher order corrections to the two main processes, since an experimental search will be able to distinguish between two-body and three-body final states. However, this is not acceptable mathematically when calculating the cross sections, due to the definition of the b sea quarks in the parton distributions for the proton and antiproton. This definition requires the subprocesses to be grouped as shown in the list above.

We will now discuss the subprocesses we have included in our calculations, subprocesses 1.1, 1.2, 2.1, 2.2, 3.1, 3.2, and 3.3, as shown in the list below. Here, the first initial state particle is a parton from the proton and the second one is a parton from the antiproton. Processes with an initial state c or s quark, or with off-diagonal CKM matrix elements are omitted from the list (and from plots) for simplicity, but have been included in our calculation of the overall cross section and other numerical results.

- | | |
|---|--|
| (1) $p\bar{p} \rightarrow t\bar{b} + X$ | |
| 1.1 | $u\bar{d} \rightarrow t\bar{b}, \bar{d}u \rightarrow t\bar{b}$ |
| 1.2 | $ug \rightarrow t\bar{b}d, gu \rightarrow t\bar{b}d, \bar{d}g \rightarrow t\bar{b}u, g\bar{d} \rightarrow t\bar{b}u$ |
| (2) $p\bar{p} \rightarrow tq + X$ | |
| 2.1 | $ub \rightarrow td, bu \rightarrow td, \bar{d}b \rightarrow t\bar{u}, b\bar{d} \rightarrow t\bar{u}$ |
| 2.2 | $ug \rightarrow td\bar{b}, gu \rightarrow td\bar{b}, \bar{d}g \rightarrow t\bar{u}\bar{b}, g\bar{d} \rightarrow t\bar{u}\bar{b}$ |
| (3) $p\bar{p} \rightarrow tW^- + X$ | |
| 3.1 | $bg \rightarrow tW, gb \rightarrow tW$ |
| 3.2 | $u\bar{u} \rightarrow tW\bar{b}, \bar{u}u \rightarrow tW\bar{b}, d\bar{d} \rightarrow tW\bar{b}, \bar{d}d \rightarrow tW\bar{b}$ |
| 3.3 | $gg \rightarrow tW\bar{b}$ |

If the initial state parton is a u quark from the proton, then contributions from both valence and sea u quarks are included in the calculations. This also applies to d quarks in

the proton and to antiquarks in the antiproton. Typical Feynman diagrams for these processes are shown in Fig. 1.

We have included in our calculations all the significant single top quark subprocesses with two or three vertices, except those with a gluon in the final state, which are significant, but which require a full next-to-leading order calculation to be included properly. Subprocesses 2.3 $bg \rightarrow tq\bar{q}'$ and 3.5 $qb \rightarrow tWq$, although they have several Feynman diagrams, only contribute 1.5% to the total $p\bar{p} \rightarrow tq + X$ cross section and 1% to the $p\bar{p} \rightarrow tW + X$ rate, respectively, and have therefore been ignored. This also applies to subprocess 3.4 $b\bar{b} \rightarrow tW\bar{b}$, despite its having multiple Feynman diagrams, including ones with electroweak $t\bar{t}$ production.

B. Calculation details

We have calculated the production cross section for each of the single top quark subprocesses mentioned in the previous section. We used the software package CompHEP [47] to do the tree level symbolic calculations and to generate optimized FORTRAN code for the squared matrix elements. Version 2.0 of CompHEP used the BASES package [48] to integrate over all phase space using parton distributions, and a CompHEP-BASES interface program to generate the correct event kinematics, with smoothing of singular variables [49]. The Monte Carlo event generator SPRING [48] was used for each process in CompHEP 2.0. CompHEP 3.0 has since replaced BASES and SPRING with VEGAS [50], and we used this version as well. Events generated were processed using PYTHIA [51] via a custom interface, in order to decay the W boson for use in kinematic studies of the final state particles.

For these calculations, we have utilized the CTEQ3M [52] and Martin-Roberts-Stirling set A' [MRS(A')] [53] parton distributions. These two sets of next-to-leading order structure functions both use the modified minimal subtraction renormalization scheme [54]. The newly available parton distributions CTEQ4M [55] and MRS(R) [56] are very similar to the distributions we have used, in the kinematic region for single top quark production at the Tevatron.

We used the following standard model parameters in our calculations: Z boson mass $m_Z = 91.19$ GeV, $\sin^2\theta_w = 0.225$, where θ_w is the weak mixing angle (giving the W boson mass $m_W = m_Z \cos\theta_w = 80.28$ GeV), b quark mass $m_b = 5.0$ GeV, $\alpha = 1/128$, and CKM matrix elements $V_{ud} = 0.975$ and $V_{tb} = 0.999$. All results have been obtained in two gauges, the unitarity gauge and the 't Hooft–Feynman gauge, as a check of calculations. Differences between calculations in the two gauges are less than 0.1%.

We have chosen to use m_t^2 as the QCD evolution parameter or scale Q^2 value, since a large scale is a natural choice for top quark production. A high value such as m_t^2 is also a conservative choice that leads to lower cross sections. As shown in Refs. [14,18], the leading order single top quark cross section depends rather strongly on the choice of QCD scale for values below $\sim (m_W/2)^2$, and if a very small value for Q^2 such as m_b^2 were to have been chosen, then the calculated cross sections would have been about four times larger than those obtained using m_t^2 .

A typical x value for single top quark processes is $\sim m_t/\sqrt{s} \approx 180/1800 = 0.1$, where x is the fraction of the

proton or antiproton momentum carried by each initial state parton. At a scale $Q^2 = (180 \text{ GeV})^2$, the value of α_s is 0.102 from CTEQ3M and 0.104 from MRS(A'). Λ_{QCD} for five quark flavors is 158.0 MeV in both CTEQ3M and MRS(A').

C. Combining cross sections

Care must be taken when combining some single top quark subprocesses in order to avoid double counting. One cannot simply add up the separate cross sections to get the total when there is a sea b quark in the initial state. The CTEQ3M and MRS(A') b sea distributions are not measured experimentally, but are obtained from the gluon distributions using the Dokshitzer-Gribov-Lipatov-Altarelli-Parisi evolution equations [57]. The b sea distributions in the structure functions therefore contain a mass singularity from the collinear divergence which occurs when the gluon splits to an on-shell $b\bar{b}$ pair. The subprocesses we are considering which pertain to this situation are 2.1 $q'b \rightarrow tq$, and 2.2 $q'g \rightarrow tq\bar{b}$ (W -gluon fusion), where the initial state b quark in subprocess 2.1 is derived from the gluon sea in the antiproton. The correct way to avoid this singularity would be to calculate the rate for subprocess 2.2 $q'g \rightarrow tq\bar{b}$ with complete loop corrections, and then subprocess 2.1 with its b sea contribution would be automatically included without the need for extracting it from the parton distribution sets. However, since we are making leading order calculations, we need another method. One technique [58,59] for obtaining the cross section $\sigma(p\bar{p} \rightarrow tq + X)$ is to calculate the rates for subprocesses 2.1 and 2.2 and add them together, and then subtract the rate from the splitting process $g \rightarrow b\bar{b}$ convolved with subprocess $q'b \rightarrow tq$. We have chosen to employ this method here. For instance, at $m_t = 180$ GeV with $Q^2 = m_t^2$ and CTEQ3M parton distributions, the naive cross section for $q'b \rightarrow tq$ is 0.75 pb, for $q'g \rightarrow tq\bar{b}$ it is 0.29 pb, and the splitting term is 0.54 pb, giving a total cross section from these two subprocesses of 0.50 pb. The rate for $p\bar{p} \rightarrow tq + X$ is thus over 70% higher than the rate from the W -gluon fusion subprocess $q'g \rightarrow tq\bar{b}$ alone.

A second subtlety [60] comes into play with this method for avoiding double counting, when working with the two parton distributions being considered: CTEQ3M and MRS(A'). The CTEQ Collaboration has chosen to evolve the b sea distribution from m_b , whereas the MRS group starts the evolution of its b sea distribution at $2m_b$. The logarithmic terms in the gluon splitting must be evaluated as $\ln(Q^2/m_b)$ with CTEQ distributions, but as $\ln(Q^2/2m_b)$ for MRS distributions, to be consistent with the respective definitions of the b quark sea.

D. Cross section versus top quark mass

We show results for the cross sections of the three electroweak single top quark processes and the totals in Fig. 2 as a function of the top quark mass, with $\sqrt{s} = 1.8$ TeV. Figure 2(a) shows $p\bar{p} \rightarrow t\bar{b} + X$, 2(b) portrays the process $p\bar{p} \rightarrow tq + X$, 2(c) is for the less important $p\bar{p} \rightarrow tW + X$ mode, and 2(d) shows the totals for each of these three pro-

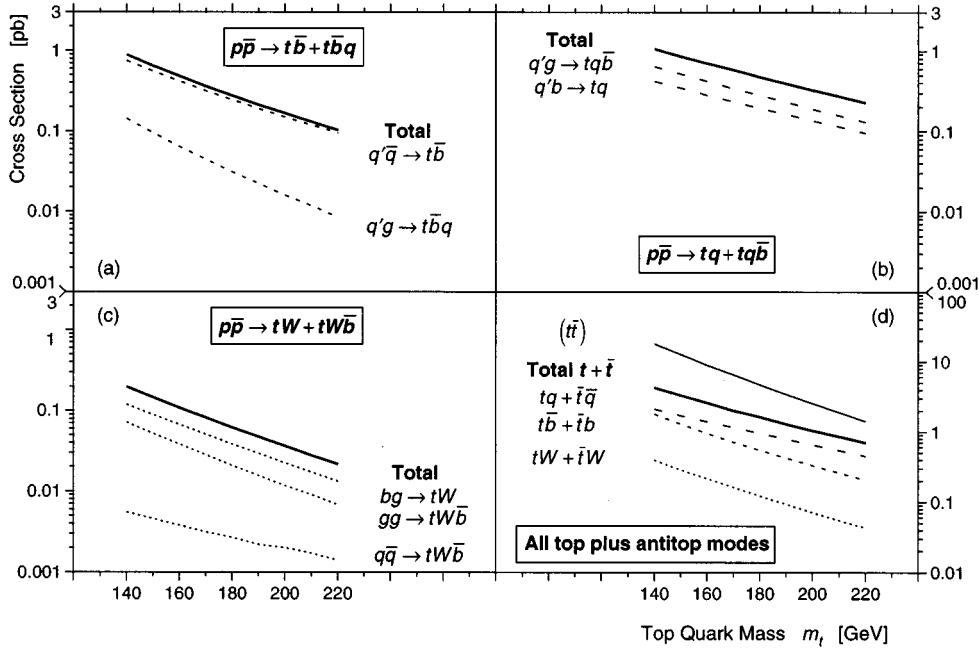


FIG. 2. Single top quark cross sections at the Tevatron with $\sqrt{s} = 1.8$ TeV, versus top quark mass: (a) s -channel W^* production $p\bar{p} \rightarrow t\bar{b} + t\bar{b}q$; (b) t - and u -channel production $p\bar{p} \rightarrow tq + tq\bar{b}$; (c) $p\bar{p} \rightarrow tW + tW\bar{b}$; and (d) the total single top quark and $t\bar{t}$ antiquark cross section $p\bar{p} \rightarrow t + \bar{t} + X$. The resummed next-to-leading order $t\bar{t}$ cross section of Ref. [61] is shown as the uppermost line in (d), for comparison with the single top quark production modes (at leading order).

cesses for t and \bar{t} combined. Figure 2(d) also shows $t\bar{t}$ pair production for comparison (upper line), and it can be seen that when only one top quark is produced in the final state, the cross sections decrease more slowly with increasing top quark mass than when two heavy top quarks have to be created at once. The strong $t\bar{t}$ cross section illustrated is from the resummed next-to-leading order calculation of Berger and Contopanagos [61], who used the CTEQ3M parton distributions. The tree level single top quark cross sections are the average of our calculations using CTEQ3M and MRS(A').

The main contribution to electroweak single top quark production comes from $p\bar{p} \rightarrow tq + X$, the W -boson t - and u -channel mode, including W -gluon fusion. The rate from this process (61%, at $m_t = 180$ GeV) is nearly twice as large as that from $p\bar{p} \rightarrow t\bar{b} + X$ with a W^* in the s channel (32%). The contribution to the total cross section of the third process $p\bar{p} \rightarrow tW + X$ is small (7%). Of the dominant t - and u -channel process, 41% of the rate comes from $q'b \rightarrow tq$ (after subtraction of the splitting term), and 59% from W -gluon fusion $q'g \rightarrow tq\bar{b}$. Therefore, W -gluon fusion forms 36% of the total single top quark rate from all processes.

Because there are contributions from several single top quark processes, the total cross section forms a significant fraction of the $t\bar{t}$ pair production rate. The single top quark and antiquark cross section from $p\bar{p}$ production at $\sqrt{s} = 1.8$ TeV is $0.92 \times 2 = 1.84$ pb for a top quark of mass 180 GeV and the CTEQ3M parton distributions, and $0.84 \times 2 = 1.68$ pb using MRS(A'). Therefore, although the rate of single top quark production is smaller than that from $t\bar{t}$ pair production (e.g., $4.71^{+0.07}_{-0.35}$ pb at 180 GeV [61]) for all top quark masses considered here, it is large enough to be extremely interesting for study at the Tevatron.

Recent calculations show that higher order corrections to the leading order single top quark cross sections presented

here are large. For instance, Ref. [17] shows that the K factor for $p\bar{p} \rightarrow tq + X$ is ~ 1.45 for $m_t = 180$ GeV at $\sqrt{s} = 1.8$ TeV with CTEQ2D parton distributions [62] and $Q^2 = m_t^2$. Reference [24] contains a similar higher order calculation for $p\bar{p} \rightarrow t\bar{b} + X$, and finds that for $m_t = 175$ GeV and $\sqrt{s} = 2.0$ TeV, the K factor is also 1.45, using the CTEQ3M parton distributions and $Q^2 = q^2$, where q^2 is the mass squared of the virtual W boson involved in this s -channel process.

E. Contributions to the single top quark cross section

Table I presents values of various partonic subprocess cross sections for a top quark of mass 180 GeV, and for the two parton distributions discussed previously. Subprocesses with an initial state strange or charm sea quark contribute 1.9% to the total $p\bar{p} \rightarrow t\bar{b} + X$ cross section, and 6.1% to the total $p\bar{p} \rightarrow tq + X$ rate. Off-diagonal CKM matrix element subprocesses (not including initial state s and c sea quark subprocesses) contribute 0.3% to $p\bar{p} \rightarrow t\bar{b} + X$ and 5.0% to $p\bar{p} \rightarrow tq + X$. All these other modes contribute $< 0.5\%$ to $p\bar{p} \rightarrow tW + X$ production. Off-diagonal CKM subprocesses and initial state s and c sea quark subprocesses are included in our calculation of the total single top quark cross section, but are not included in our plots for simplicity, because of the calculation technique used.

For single top quark modes such as W^* s -channel production with only light partons in the initial state, including both valence and sea quarks, the cross sections calculated with MRS(A') are 2.4% lower than those calculated with CTEQ3M. When there is a gluon in the initial state, for instance in W -gluon fusion, then the MRS(A') cross sections are 5.7% lower than the CTEQ3M ones. For reactions with a b sea quark in the initial state, the cross sections calculated with MRS(A') are 17% smaller.

Table II shows the resulting single top quark cross sections as a function of top quark mass. The central value

TABLE I. Production cross sections for single top quark processes for $m_t=180$ GeV, with $Q^2=m_t^2$ and $\sqrt{s}=1.8$ TeV, using CTEQ3M and MRS(A') parton distributions. "Other modes" refers to subprocesses with an s or c quark in the initial state, and to subprocesses involving an off-diagonal CKM matrix element term.

Single top quark production process	Cross section [pb]	
	CTEQ3M	MRS(A')
(1) $p\bar{p}\rightarrow t\bar{b}+X$	0.2847	0.2772
1.1 $q'\bar{q}\rightarrow t\bar{b}$	0.2510	0.2452
$u\bar{d}\rightarrow t\bar{b}$	0.2423	0.2370
$\bar{d}u\rightarrow t\bar{b}$	0.0044	0.0040
Other modes	0.0043	0.0042
1.2 $q'g\rightarrow t\bar{b}q$	0.0337	0.0320
$ug\rightarrow t\bar{b}d$	0.0213	0.0200
$gu\rightarrow t\bar{b}d$	0.0009	0.0009
$\bar{d}g\rightarrow t\bar{b}\bar{u}$	0.0016	0.0015
$g\bar{d}\rightarrow t\bar{b}\bar{u}$	0.0080	0.0077
Other modes	0.0019	0.0019
(2) $p\bar{p}\rightarrow tq+X$	0.5697	0.5059
2.1 $q'b\rightarrow tq$	0.2448	0.2013
$ub\rightarrow td$	0.1607	0.1333
$bu\rightarrow td$	0.0063	0.0048
$\bar{d}b\rightarrow t\bar{u}$	0.0075	0.0056
$b\bar{d}\rightarrow t\bar{u}$	0.0403	0.0338
Other modes	0.0300	0.0238
2.2 $q'g\rightarrow tq\bar{b}$	0.3249	0.3046
$ug\rightarrow t\bar{d}\bar{b}$	0.2162	0.2034
$gu\rightarrow t\bar{d}\bar{b}$	0.0080	0.0073
$\bar{d}g\rightarrow t\bar{u}\bar{b}$	0.0100	0.0089
$g\bar{d}\rightarrow t\bar{u}\bar{b}$	0.0559	0.0540
Other modes	0.0348	0.0310
(3) $p\bar{p}\rightarrow tW+X$	0.0658	0.0573
3.1 $bg\rightarrow tW$	0.0418	0.0346
$bg\rightarrow tW$	0.0209	0.0173
$gb\rightarrow tW$	0.0209	0.0173
3.2 $q\bar{q}\rightarrow tW\bar{b}$	0.0027	0.0026
$u\bar{u}\rightarrow tW\bar{b}$	0.0024	0.0023
$\bar{u}u\rightarrow tW\bar{b}$	0.0000	0.0000
$d\bar{d}\rightarrow tW\bar{b}$	0.0003	0.0003
$\bar{d}d\rightarrow tW\bar{b}$	0.0000	0.0000
3.3 $gg\rightarrow tW\bar{b}$	0.0213	0.0201
$\sigma(p\bar{p}\rightarrow t+X)$	0.9202	0.8404

numbers are the mean of the values calculated using CTEQ3M and MRS(A'). The upper and lower bounds come from combining one-half the difference between the calculations using the two parton distributions with the errors from the choice of QCD scale, as discussed in the next section. The correlation of the errors is correctly accounted for by adding the Q^2 errors to each subprocess separately, before adding them in quadrature with the uncertainty due to the choice of structure function. For a top quark of mass

180 GeV, the total single top quark plus antiquark cross section is $1.76^{+0.26}_{-0.18}$ pb.

F. Cross section versus scale

We have examined the effect of the choice of QCD evolution parameter Q^2 on the various single top quark subprocesses. The results are shown in Fig. 3 for a top quark of mass 180 GeV and the CTEQ3M parton distributions at $\sqrt{s}=1.8$ TeV. Figure 3(a) shows the scale dependence for the W^* s -channel process $p\bar{p}\rightarrow t\bar{b}+X$, which is the least dependent of the various single top quark processes on the choice of scale. Figure 3(b) is for the t - and u -channel processes $q'g\rightarrow tq\bar{b}$ (W -gluon fusion) and $q'b\rightarrow tq$. The W -gluon fusion cross section falls rapidly as the calculation scale increases, whereas the subprocess $q'b\rightarrow tq$ goes up as Q^2 is raised. When these subprocesses are combined, the two effects partially cancel. The $q'b\rightarrow tq$ subprocess is shown with the $g\rightarrow b\bar{b}$ splitting term already subtracted. The minor single top quark process $p\bar{p}\rightarrow tW+X$ is shown in Fig. 3(c) with its various contributing subprocesses, which again have differing dependences on Q^2 that partially cancel in the sum. Finally, Fig. 3(d) shows each single top quark process summed for t and \bar{t} , and the total single top quark production on the same axis for comparison.

Leading order cross sections show more sensitivity to the choice of scale than those from higher order calculations. However, one still needs to choose a scale at which to perform the calculations. From an intuitive perspective, it does not make sense to consider top quark production as occurring at the almost zero mass b quark scale, although it would be mathematically consistent. Therefore, for our calculations, we have chosen the central value of the scale to be $Q^2=m_t^2$, and when estimating the uncertainty due to the choice of scale, we have restricted the region of interest to lie between $(m_t/2)^2$ and $(2m_t)^2$, as shown on the upper axes of Fig. 3. The resulting errors on the main contributions to the cross section at $m_t=180$ GeV are: $^{+9}_{-11}\%$ for $p\bar{p}\rightarrow t\bar{b}+X$; $^{+8}_{-9}\%$ for $q'b\rightarrow tq$ and $^{+32}_{-20}\%$ for $q'g\rightarrow tq\bar{b}$, which combine to give $^{+15}_{-8}\%$ for $p\bar{p}\rightarrow tq+X$; and $^{+29}_{-14}\%$ for $p\bar{p}\rightarrow tW+X$. The $q'b\rightarrow tq$ and $q'g\rightarrow tq\bar{b}$ errors largely cancel because the contributions to the errors from choice of Q^2 are 100% anticorrelated. The Q^2 scale error dominates the total errors on the cross sections given in Table II.

Combining the subprocesses $q'b\rightarrow tq$ and $q'g\rightarrow tq\bar{b}$ by subtracting the gluon splitting term to avoid double counting, as discussed earlier, is a procedure that is sensitive to the choice of evolution parameter Q^2 . Figure 4 shows the subprocess $q'b\rightarrow tq$ before and after subtraction, as a function of (a) the top quark mass, and (b) the scale Q^2 . It can be seen however, that provided the scale remains in the region around m_t^2 , then the sensitivity is less than that seen for the W -gluon fusion subprocess $q'g\rightarrow tq\bar{b}$ in Fig. 3(b).

G. Cross section versus collider energy

We have calculated the single top quark cross section as a function of production energy \sqrt{s} . Figure 5(a) shows the cross section versus top quark mass for four collision ener-

TABLE II. Single top quark plus antiquark cross sections at the Tevatron with $\sqrt{s}=1.8$ TeV and $Q^2=m_t^2$, as a function of top quark mass. The central values are the mean of the calculations using CTEQ3M and MRS(A'). The upper and lower bounds include the effects from choice of scale Q^2 and one-half the difference between the parton distribution functions.

Total single top quark cross section [pb]									
m_t [GeV]	$\sigma(p\bar{p}\rightarrow t+\bar{t}+X)$			(1) $\sigma(p\bar{p}\rightarrow t\bar{b}+\bar{t}b+X)$			(3) $\sigma(p\bar{p}\rightarrow tW+\bar{t}W+X)$		
	Lower bound	Central value	Upper bound	Lower bound	Central value	Upper bound	Lower bound	Central value	Upper bound
140	4.15	4.61	5.19	1.70	1.83	2.02	0.32	0.39	0.48
150	3.20	3.56	4.03	1.21	1.33	1.45	0.24	0.29	0.36
160	2.51	2.79	3.17	0.88	0.98	1.07	0.18	0.22	0.28
170	1.98	2.21	2.52	0.66	0.74	0.80	0.14	0.16	0.21
180	1.58	1.76	2.02	0.50	0.56	0.61	0.10	0.12	0.16
190	1.26	1.42	1.63	0.39	0.43	0.47	0.08	0.09	0.12
200	1.02	1.15	1.32	0.30	0.34	0.37	0.06	0.07	0.09
210	0.83	0.93	1.07	0.24	0.27	0.30	0.04	0.06	0.07
220	0.67	0.76	0.88	0.19	0.21	0.24	0.03	0.04	0.05

m_t [GeV]	2.1 $\sigma(q'\bar{b}\rightarrow tq,\bar{q}'\bar{b}\rightarrow\bar{t}\bar{q})$			2.2 $\sigma(q'g\rightarrow tq\bar{b},\bar{q}'g\rightarrow\bar{t}\bar{q}b)$			(2) $\sigma(p\bar{p}\rightarrow tq+\bar{t}\bar{q}+X)$		
	Lower bound	Central value	Upper bound	Lower bound	Central value	Upper bound	Lower bound	Central value	Upper bound
140	0.85	0.95	1.07	1.13	1.43	1.81	2.13	2.38	2.69
150	0.69	0.78	0.88	0.92	1.16	1.49	1.75	1.94	2.22
160	0.57	0.65	0.73	0.75	0.94	1.23	1.44	1.59	1.83
170	0.47	0.54	0.60	0.62	0.77	1.01	1.18	1.31	1.51
180	0.39	0.45	0.50	0.50	0.63	0.83	0.97	1.08	1.25
190	0.32	0.37	0.42	0.41	0.52	0.68	0.80	0.89	1.03
200	0.27	0.31	0.35	0.34	0.43	0.56	0.66	0.74	0.86
210	0.23	0.26	0.29	0.28	0.35	0.46	0.54	0.61	0.71
220	0.19	0.22	0.25	0.22	0.29	0.38	0.44	0.51	0.58

gies: (i) the current Tevatron energy 1.8 TeV; (ii) the Tevatron energy for the next run in 1999, 2.0 TeV; (iii) the energy of a possible Tevatron upgrade, 4.0 TeV; and (iv) the energy of the Large Hadron Collider (LHC) at CERN in 2005, 14 TeV. The three Tevatron cross sections are for $p\bar{p}$ collisions, whereas the LHC cross sections are calculated for pp collisions. Despite the $\sim 150\times$ increase in cross sections at the LHC, it will still be rather difficult to study single top quark production there, since the backgrounds will be much larger, and the signal will be harder to identify, because the jet produced at the same time as the top quark in W -gluon fusion, for instance, will be further forward in pseudorapidity η , where $\eta=\ln \tan(\theta/2)$ and θ is the polar angle between the jet and the proton beamline. Peaks in the accompanying jet distribution at the LHC will occur at $\eta=\pm 2.5$ (cf. η peaks at ± 1.5 when $\sqrt{s}=1.8$ TeV).

At $m_t=180$ GeV, the cross section for single top quark production is 0.85 pb at 1.8 TeV, 1.4 pb at 2.0 TeV, 9.4 pb at 4.0 TeV, and for pp collisions at 14 TeV, 179 pb. For 180 GeV \bar{t} antiquarks, the cross sections are the same as those for t quarks at the Tevatron, but only 133 pb at the LHC (26% lower), because there are no valence antiquarks in the initial state. These calculations were done using the CTEQ3M parton distributions with $Q^2=m_t^2$, and no contri-

butions from initial state s or c quarks or off-diagonal CKM matrix element terms are included.

The relative contributions to the total single top quark cross section from each of the significant processes are not the same at all production energies. For a top quark of mass 180 GeV, Fig. 5(b) shows the single top quark plus top antiquark cross section versus production energy at the Tevatron for each component of the signal separately. It can be seen that the W^* s -channel process $p\bar{p}\rightarrow t\bar{b}+\bar{t}b+X$ is much less sensitive to the change in available energy than are the other processes, which increase rapidly in rate as the initial state energy goes up. At $\sqrt{s}=1.8$ TeV, the W^* process forms 32% of the total single top quark signal, at 2.0 TeV it provides 29% of the cross section, and by 4.0 TeV it contributes only 13%. The $p\bar{p}\rightarrow t\bar{b}+\bar{t}b+X$ process behaves in this manner because it is an s -channel process and its contribution to the total cross section comes from the \hat{s} threshold phase space region, which is independent of energy. The reason why the total cross section increases with energy is that at higher energies, regions of smaller x in the proton structure functions are probed, and this is where the parton distributions are larger.

The contribution from $p\bar{p}\rightarrow tW+X$ to the total single top quark cross section increases from 7% at $\sqrt{s}=1.8$ TeV

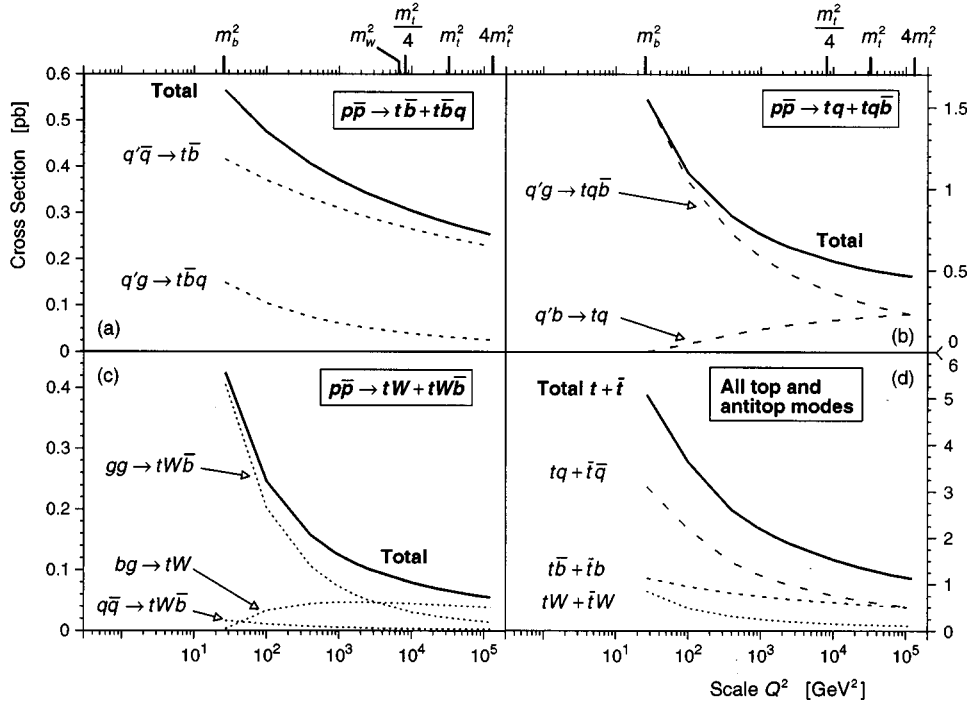


FIG. 3. Single top quark cross sections ($m_t=180$ GeV, $\sqrt{s}=1.8$ TeV) versus QCD evolution scale Q^2 for: (a) s -channel W^* production $p\bar{p}\rightarrow t\bar{b}+t\bar{b}q$; (b) t - and u -channel production $p\bar{p}\rightarrow tq+ tq\bar{b}$; (c) $p\bar{p}\rightarrow tW+tW\bar{b}$; and (d) the summed single top quark and \bar{t} antiquark cross section $p\bar{p}\rightarrow t+\bar{t}+X$.

through 9% at 2.0 TeV, to 20% at 4.0 TeV. At the LHC, $pp\rightarrow tW+X$ will contribute 30% of the single top quark rate and 40% of the \bar{t} antiquark rate, and could therefore be an important production mode in the future. On the other hand, at the LHC, the s -channel process $pp\rightarrow t\bar{b}+\bar{t}b+X$ will fall to only 5% of the total single top quark rate, and will become experimentally inaccessible.

H. A closer look at W -gluon fusion

We have analyzed the contributions to the production rate from the two Feynman diagrams which form W -gluon fusion $q'g\rightarrow tq\bar{b}$, shown in Fig. 6(a). There is no interference between the W -gluon fusion diagrams and the two nonfusion

diagrams of subprocess $q'g\rightarrow t\bar{b}q$ [shown in Fig. 1(a) as subprocess 1.2], because the final state t quark and \bar{b} antiquark have a different color structure. For the nonfusion diagrams, the t and \bar{b} are from a W decay and so are in a color singlet state, whereas for the fusion diagrams the t and \bar{b} come from a gluon and so are in a color octet state.

The contribution to the total production rate of W -gluon fusion from the Feynman diagram where the gluon produces a $t\bar{t}$ pair is very small, at about 5%. However, this diagram interferes destructively with the main W -gluon fusion diagram where $g\rightarrow b\bar{b}$. The destructive interference reduces the total rate for W -gluon fusion by 34%. We present the cross section versus top quark mass for the two diagrams of

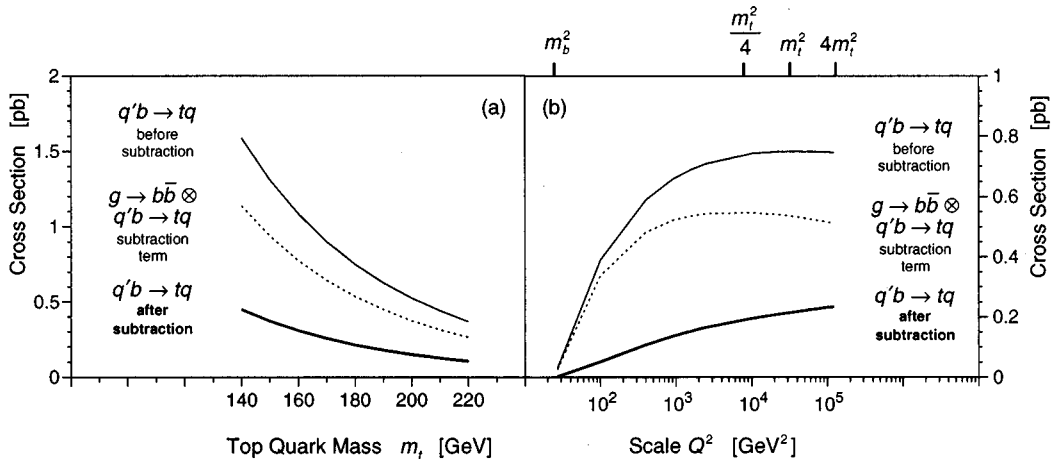


FIG. 4. A single top quark produced together with a light quark, $q'b\rightarrow tq$, from an initial state b sea quark, showing the cross section before and after subtraction of the gluon splitting term, as a function of: (a) top quark mass (with $Q^2=m_t^2$); and (b) scale Q^2 (with $m_t=180$ GeV).

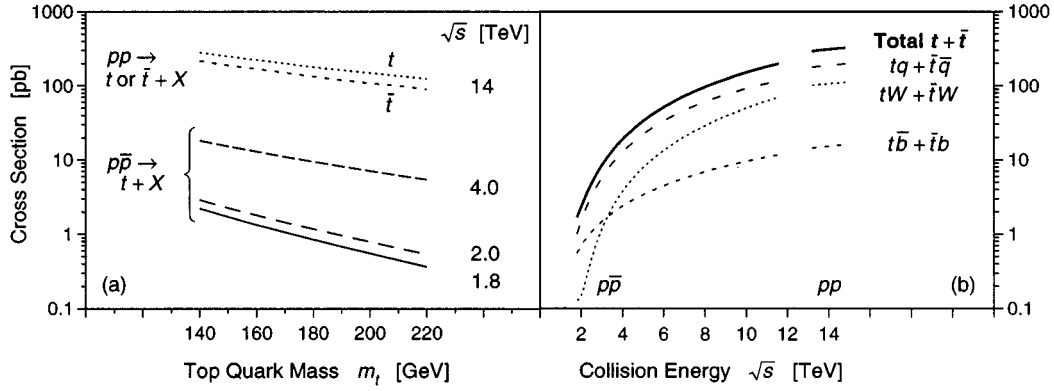


FIG. 5. Single top quark cross section plotted (a) versus top quark mass, at four production energies: the Fermilab Tevatron at $\sqrt{s} = 1.8$ TeV; the upgraded Tevatron at 2.0 TeV; the proposed TeV* collider at 4.0 TeV; and the CERN pp Large Hadron Collider at 14 TeV. Plot (b) shows the cross section versus collider energy (with $m_t = 180$ GeV), for each of the single top quark production mechanisms. The values in (b) up to 12 TeV are for $p\bar{p}$ production, whereas the results at 14 TeV are for pp collisions.

W -gluon fusion separately, and show the interference and net result, in Fig. 6(b).

I. More on $p\bar{p} \rightarrow tW + X$

We have considered two related $2 \rightarrow 3$ body processes in addition to the process $bg \rightarrow tW$. These are $q\bar{q} \rightarrow tW\bar{b}$ and $g\bar{g} \rightarrow tW\bar{b}$. We looked at these processes because in e^+e^- and $\gamma\gamma$ colliders, single top quark processes with $tW\bar{b}$ in the final state are important. However, we found that at the Tevatron these processes are not very significant. The interactions e^+e^- , $\gamma\gamma$, $q\bar{q}$, and $g\bar{g} \rightarrow tW\bar{b}$ all include diagrams with $t\bar{t}$ pair production and subsequent decay of the \bar{t} into $W\bar{b}$, as well as many additional diagrams with just single top quark production. One needs to remove the contribution to the cross section from the invariant mass region $m_t = m_{Wb}$ around the top quark pole in order to study the Wtb vertex in single top quark production. The remaining contributions in e^+e^- and $\gamma\gamma$ collisions are large enough (at 10 fb which is 17% of the total $tW\bar{b}$ cross section for e^+e^- collisions at $\sqrt{s} = 2$ TeV, for example) to be sensitive to the coupling structure, but in $q\bar{q}$ and $g\bar{g}$ collisions almost the entire cross

section comes from the $t\bar{t}$ diagrams, and the remaining single top quark contribution at 29 fb, is only $\sim 0.8\%$ of the total $tW\bar{b}$ rate of 3.5 pb.

II. KINEMATIC DISTRIBUTIONS

In order to understand in more detail the properties of single top quark production, we present in this section several experimentally interesting kinematic distributions. These are shown for top quark production only (not \bar{t}) to make the presentation clear. Distributions for \bar{t} antiquarks are the same as those for top quarks in transverse momentum, but are mirror images in pseudorapidity. If the sign of the W -boson charge can be measured using its leptonic decay modes, then it will be possible to study the properties of top quarks and \bar{t} antiquarks separately. All plots are for a top quark of mass 180 GeV and have been calculated using the CTEQ3M parton distributions at $\sqrt{s} = 1.8$ TeV.

The top quark decays to a W^+ boson and a b quark, and we consider here only subsequent leptonic decays of the W to a positron and neutrino, as this signal should be easier to find experimentally than channels with hadronic decay of the W boson. The branching fraction B for this decay mode is

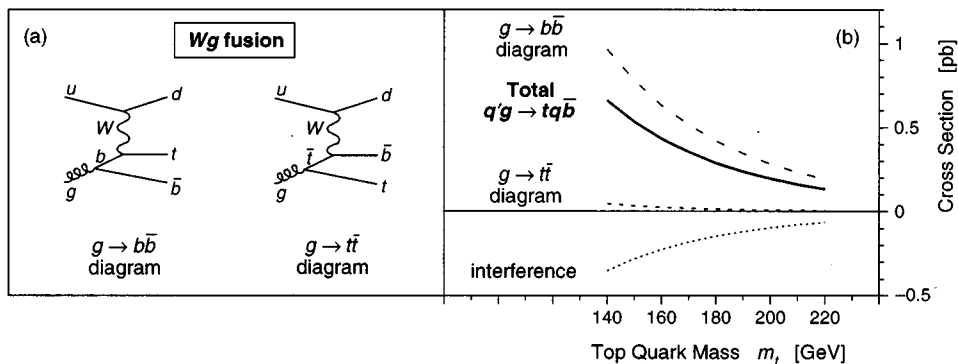


FIG. 6. (a) Feynman diagrams for W -gluon fusion ($q'g \rightarrow tq\bar{b}$). (b) W -gluon fusion cross section versus top quark mass, showing the contributions from each of the Feynman diagrams, and the large destructive interference between the two processes.

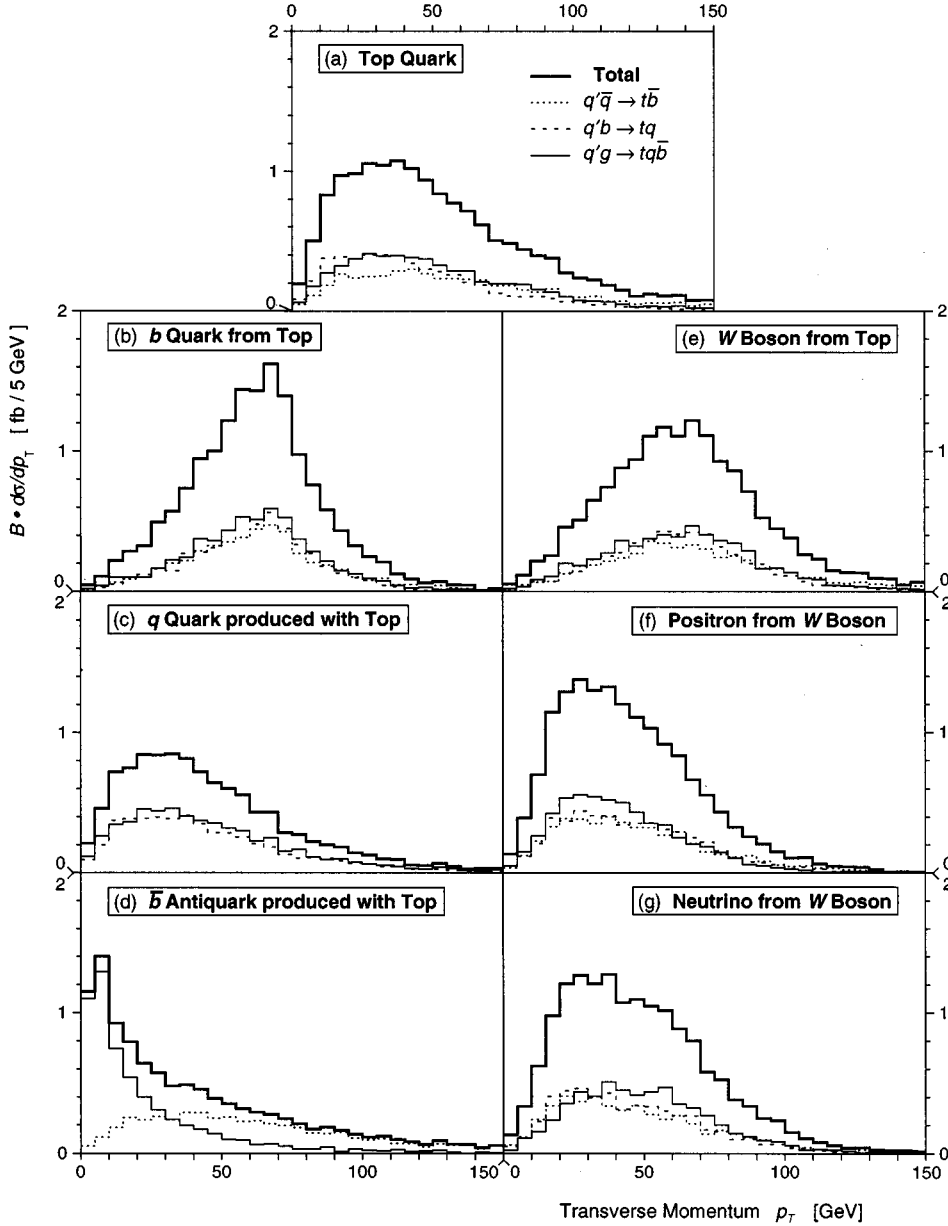


FIG. 7. Transverse momentum distributions in single top quark events (with $m_t=180$ GeV) for: (a) the top quark; (b) the b quark from the decay of the top quark; (c) the light q quark produced with the top quark in the t - and u -channel processes; (d) the \bar{b} antiquark produced with the top quark in the s -channel W^* process, and in W -gluon fusion; (e) the W boson from the top quark decay; (f) the positron from the W decay; and (g) the neutrino also from the decay of the W boson.

$\frac{1}{9}$. The signature for a single top quark event is therefore a central, isolated, high p_T lepton, large missing transverse momentum from the neutrino, and at least two jets, where one of the jets comes from the hadronization of the b quark from the decay of the top quark. All single top quark events therefore have one potentially identifiable b jet, and of the experimentally accessible production modes at the Tevatron ($p\bar{p} \rightarrow t\bar{b} + X, tq + X$), $\sim 71\%$ of them have a \bar{b} jet as well.

A. Transverse momentum

Figure 7 shows the branching fraction times differential cross section $B \cdot d\sigma/dp_T$ versus transverse momentum p_T of the final state partons in single top quark production, and their decay products. In each plot, the short-dashed line is for W^* production $q'\bar{q} \rightarrow t\bar{b}$, the long-dashed line for the two-body t -channel process $q'b \rightarrow tq$, and the narrow solid line for W -gluon fusion $q'g \rightarrow tq\bar{b}$. The wide solid line is the

sum of these three processes. Plot 7(a) shows the transverse momentum distributions of the top quark from each single top quark process. The mean of these distributions is 51 GeV. Despite its very high mass, the top quark is not produced at rest, but carries considerable transverse momentum in all three production modes. When the top quark decays, it produces a b quark, whose p_T distribution is shown in plot 7(b). The mean p_T here is 62 GeV. Plot 7(c) is for the light quark produced with the top quark in the t -channel processes ($\langle p_T \rangle = 43$ GeV), and 7(d) is for the \bar{b} antiquark often produced with the top quark. Here, the \bar{b} from W^* single top quark production has $\langle p_T \rangle = 59$ GeV, whereas the \bar{b} in W -gluon fusion is much softer, with $\langle p_T \rangle = 25$ GeV. The low p_T will make this jet much more difficult to reconstruct. When the top quark decays, it produces a W boson, whose p_T is shown in Fig. 7(e) ($\langle p_T \rangle = 65$ GeV). The W decays to a positron [shown in Fig. 7(f)] with mean p_T of 45 GeV and a neutrino [in Fig. 7(g), 48 GeV].

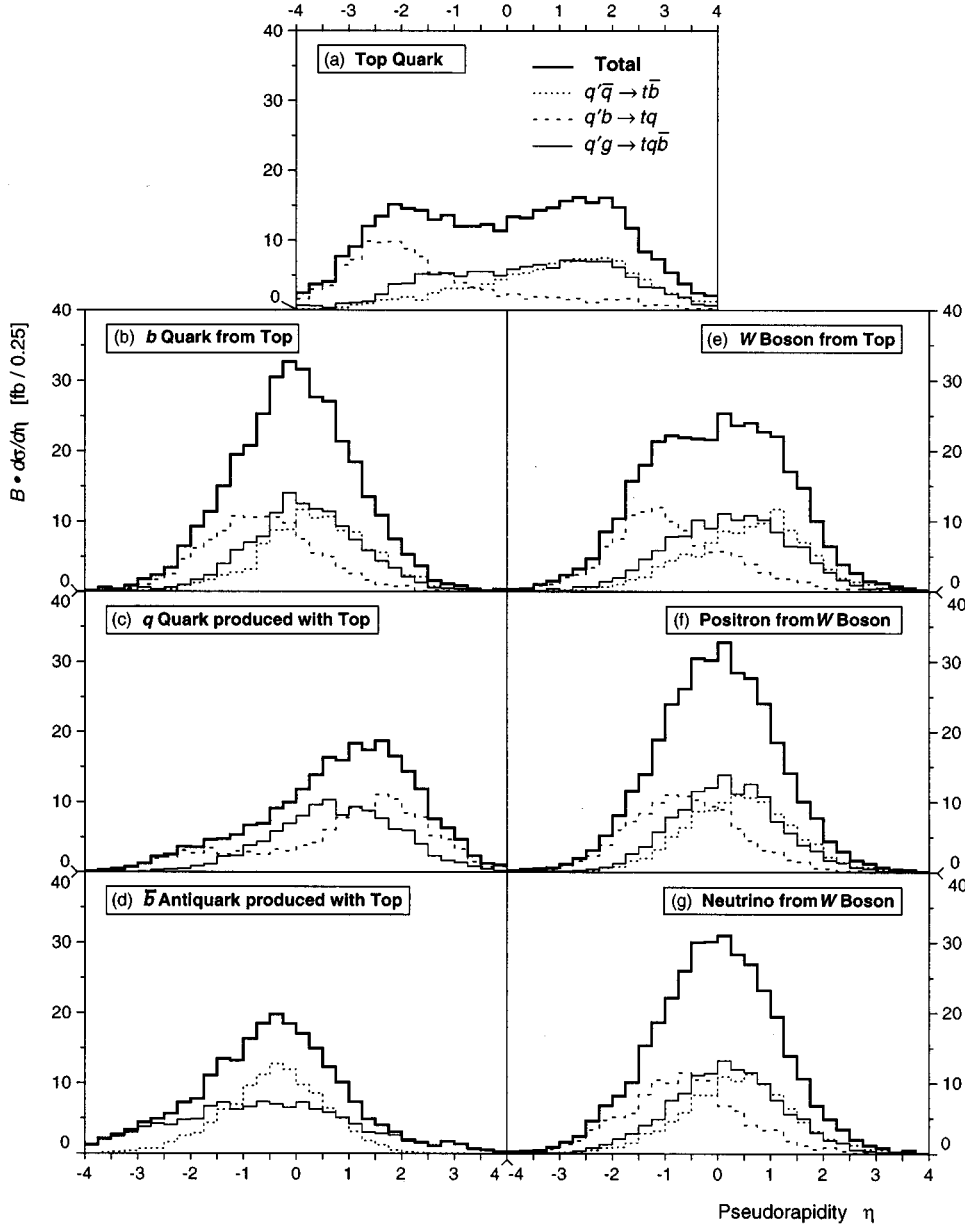


FIG. 8. Pseudorapidity distributions (with $m_t = 180$ GeV) for: (a) the top quark; (b) the b quark from the decay of the top quark; (c) the light q quark produced with the top quark in the t - and u -channel processes; (d) the \bar{b} antiquark produced with the top quark in the s -channel W^* process, and in W -gluon fusion; (e) the W boson from the top quark decay; (f) the positron from the W decay; and (g) the neutrino also from the decay of the W boson.

B. Pseudorapidity

Figure 8 shows the branching fraction times differential cross section $B \cdot d\sigma/d\eta$ versus pseudorapidity η of the final state partons from single top quark production, and their decay products. Plot 8(a) is for the top quark itself, where one can see that the pseudorapidity distributions are rather broad, and that the contributing production modes have very different kinematics from one another. Both the W -gluon fusion and W^* modes produce top quarks more in the forward or $+\eta$ direction than backwards (with the distributions peaked at $\eta \sim 1.7$) whereas the two-body t -channel process $q'b \rightarrow tq$ produces mainly backwards traveling top quarks, with the peak at $\eta \sim -2.3$. This distribution is also narrower than the other two. We see next that the decay products from the top quark are produced much more centrally. Plot 8(b) shows the b quark pseudorapidities. The distribution for the b from top quark decay in W -gluon fusion is peaked at $\eta \sim 0.1$, and the b from t in W^* production is at ~ 0.2 . The b from the top quark in $q'b \rightarrow tq$ is still produced somewhat backwards,

with a peak at ~ -0.8 reflecting the direction of its parent. We would like to note that the η distribution of the b quark from the top quark decay in W -gluon fusion is in agreement with that seen by Yuan using the ONETOP generator [11], but is rather different from the distribution for W -gluon fusion shown in the TeV-2000 study of $WH, H \rightarrow b\bar{b}$ [63] (with single top production as a background), where the HERWIG generator [64] was used for this single top quark mode. HERWIG seems to produce b 's in a symmetric peak in the region $1 < |\eta| < 5$. This difference is not understood.

One of the striking features of W -gluon fusion is the forward direction in which the light quark is produced [11]. This can be seen in plot 8(c), where the light quark from $q'g \rightarrow tq\bar{b}$ has a broad distribution, peaked at ~ 0.7 . The effect is seen more emphatically in the two-body t -channel mode where the peak occurs around 1.7, resulting in the summed distribution peaking at $\eta \sim 1.5$. The pseudorapidity distributions of the \bar{b} antiquark produced together with the

top quark in 71% of single top events are shown in plot 8(d). Both distributions peak at $\eta \sim -0.4$; the soft \bar{b} from W -gluon fusion has a rather broad spread in pseudorapidity, whereas the much harder \bar{b} from W^* production is produced in a narrower pseudorapidity peak. The η distributions of the W boson from the decay of the top quark, shown in plot 8(e), are peaked at ~ 0.3 for W -gluon fusion, at ~ 1.1 for W^* production, and at ~ -1.2 for the $q'b \rightarrow tq$ mode, echoing the directions of their respective parent top quarks. The positron [Fig. 8(f)] and neutrino [Fig. 8(g)] distributions are more central versions of their parent W bosons.

III. Wtb COUPLING AND V_{tb}

Since the top quark is rather heavy, we expect that new physics might be revealed at the scale of its mass. Many variants of nonstandard physics relating to this subject have been considered in the literature. Possible anomalous gluon-top quark couplings are discussed in Refs. [65–71]. Contact terms and new strong dynamics involving the top quark have been studied in [72–77]. The Ztt coupling will be inaccessible until a high energy e^+e^- or $\mu^+\mu^-$ collider is in operation. Studies of the Wtb coupling, however, will be possible before then using single top quark production at the Tevatron.

In this section we examine the effects on single top quark production and on its decay kinematics of a deviation in the Wtb coupling from the standard model structure, and we consider how this will affect a measurement of the CKM matrix element V_{tb} . In the standard model, the Wtb coupling is proportional to V_{tb} and has $(V-A)$ structure. As explained in the Introduction, the cross section for single top quarks includes the Wtb coupling directly, in contrast with $t\bar{t}$ pair production. Therefore, single top quark production provides a unique opportunity to study the Wtb structure and to measure V_{tb} . Experimental studies of this type are among the main goals of single top quark physics. Because high statistics will be required to make sensitive measurements, all the results given in the remaining subsections of this paper are for single top events produced in Runs 2 or 3 of the Tevatron; that is, from 1999 onwards, with a collision energy of $\sqrt{s} = 2.0$ TeV.

A. Anomalous $(V+A)$ coupling

As an example of a deviation from the standard model Wtb coupling, we introduce an additional contribution from a nonstandard $(V+A)$ structure with an arbitrary parameter A_r , where the subscript r refers to the right-handed current it represents. In the unitarity gauge, the Wtb coupling is given by

$$\Gamma = \frac{eV_{tb}}{2\sqrt{2}\sin\theta_w} [\gamma_\mu(1-\gamma_5) + A_r\gamma_\mu(1+\gamma_5)],$$

where e is the positron electric charge, $\sin\theta_w = 0.474$, and γ_μ and γ_5 are Dirac matrices.

The dependence of the total single top quark cross section on the parameter A_r is shown in Fig. 9, for $\sqrt{s} = 2.0$ TeV, $m_t = 180$ GeV, and $V_{tb} = 0.999$. Here, $\sigma(p\bar{p} \rightarrow t$

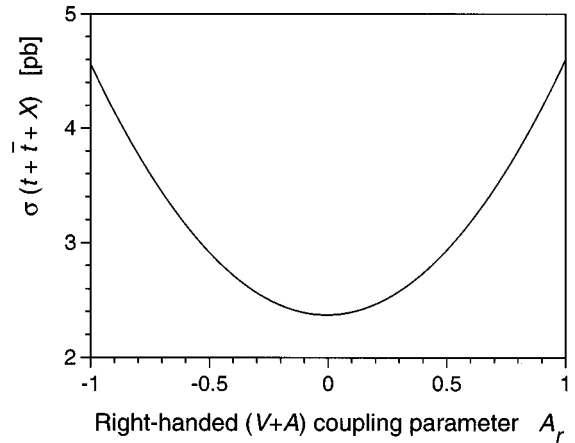


FIG. 9. Total single top quark and \bar{t} antiquark production cross section at the upgraded Tevatron, with $\sqrt{s} = 2.0$ TeV and $m_t = 180$ GeV, versus the right-handed $(V+A)$ coupling parameter A_r .

$+ \bar{t} + X) = 2 \times \sigma(p\bar{p} \rightarrow t\bar{b} + tq + tq\bar{b})$. The standard model value of A_r is zero. The production rate varies almost quadratically with A_r , and is nearly symmetric about the point $A_r = 0$. The cross section rises from 2.44 pb when $A_r = 0$ to 4.68 pb when $A_r = -1$ and to 4.73 pb when $A_r = +1$.

B. Sensitivity in the (V_{tb}, A_r) plane

We have calculated the region in the (V_{tb}, A_r) plane for which there will be experimental sensitivity using future single top quark measurements. If one finds a number of single top quark events consistent with the standard model prediction, then it may be that the Wtb coupling is purely left handed, and that V_{tb} is close to unity. Alternatively, the cross section could be boosted by an anomalous contribution to the Wtb coupling, as shown for example in Fig. 9, with V_{tb} correspondingly lower.

The error on the measurement of V_{tb} is dependent on the error on the single top quark cross section, including both experimental and theoretical contributions. First, we estimate the experimental error for a top quark of mass 180 GeV at $\sqrt{s} = 2.0$ TeV as follows: we take the integrated luminosity for Tevatron Run 2 as 2 fb^{-1} , with an error of 5%; the signal acceptance including at least one b tag as 0.20, from the TeV-2000 study of single top quark production [78], with an error of 7%; and a signal to background ratio of 1:2, with a systematic error on the background of 7%. The available branching fraction includes both the electron and muon decay channels, giving $B = \frac{2}{9}$. In Run 2, all accessible modes of single top quark production will have to be used together in order not to make a statistics-limited measurement. We use here the value 2.44 pb for the single top quark cross section [$= 0.72 \text{ pb}$ (s channel) $+ 1.72 \text{ pb}$ (t and u channels)] from CTEQ3M. These assumptions lead to a prediction that approximately 650 events will be found in a search, with one-third coming from single top quark production and two-thirds from various backgrounds (e.g., $W + b\bar{b}$, $W +$ light jets with a mistag, and $t\bar{t}$). Therefore, the experimental error on the total single top quark cross section will be 10% (statistical) \oplus 16% (systematic) = 19%, where the \oplus symbol means “add in quadrature.”

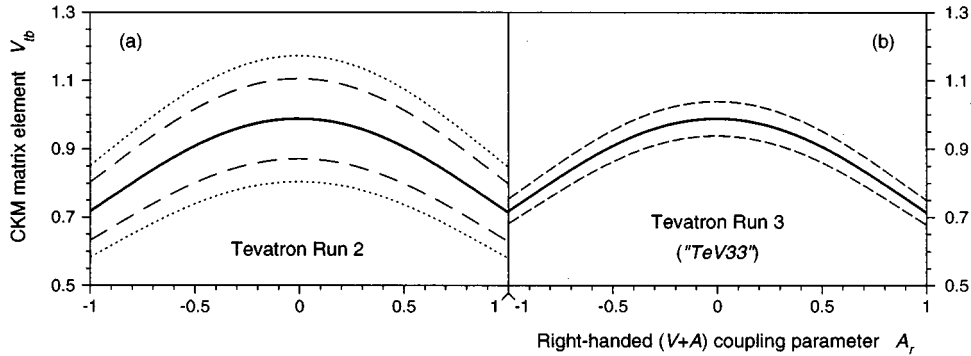


FIG. 10. Estimated 1σ measurements in the (V_{tb}, A_r) plane for an experiment running at the upgraded Tevatron collider at $\sqrt{s}=2.0$ TeV, assuming that the number of events seen is consistent with the standard model prediction. Plot (a) shows the results for 2 fb^{-1} of data, using all accessible modes of single top quark production ($p\bar{p}\rightarrow t\bar{b}+tq+tq\bar{b}+\text{c.c.}$). The outer short-dashed lines enclose the region resulting from a 32% error on the theoretical cross section and the inner long-dashed lines from a 16% uncertainty. Plot (b) is for a future run with 30 fb^{-1} of data, using only W^* single top quark production ($p\bar{p}\rightarrow t\bar{b}+\bar{t}b+X$) where the error on the theoretical cross section is 3%.

The error on the theoretical calculation of the cross section includes contributions from the choice of parton distribution function and from the scale, as discussed earlier in this paper, where they were found to be $\sim 12\%$. However, there is another contribution, not well quantified, from the lack of knowledge of the gluon distribution in the proton and antiproton for t - and u -channel single top quark processes. This error has been variously reported to us as 30% [79] and 10% [80], and so we use these values here to estimate the error on the theoretical total single top quark cross section at 32% or 16%.

The error on a measurement of V_{tb} will be one-half the error on the single top quark cross section, since the cross sections for all single top quark processes are proportional to $|V_{tb}|^2$. This results in an error on V_{tb} of $(19\% \oplus 32\%)/2 = 19\%$ or $(19\% \oplus 16\%)/2 = 12\%$ from the Tevatron Run 2, depending on one's view of the knowledge of the gluon momentum distributions in the proton sea.

There may be a Run 3 at the Tevatron from 2002 onwards, producing 30 fb^{-1} of data. This high luminosity mode of collider running is known as ‘‘TeV33’’ after the planned instantaneous luminosity of $10^{33}\text{ cm}^{-2}\text{ s}^{-1}$. With such high statistics available, it has been shown by Stelzer and Willenbrock [22] that using just s -channel W^* production with double b tagging instead of all single top quark modes with only one tag will eliminate most of the uncertainty on the theoretical cross section, because there will no longer be any contributions from processes with initial state gluons. They also showed that the measurement should be possible using 3 fb^{-1} of data. We update their calculation here for Run 3, including estimates of the systematic errors. The cross section for $p\bar{p}\rightarrow t\bar{b}+\bar{t}b+X$ is 0.716 pb , with $m_t=180\text{ GeV}$, $\sqrt{s}=2.0\text{ TeV}$, and $Q^2=m_t^2$. To estimate the error on V_{tb} using Run 3 data, we make the following assumptions: the error on the luminosity remains at 5%; the signal acceptance for W^* single top quark production is 0.08 when requiring a double b tag, as shown in Ref. [22], with a 1.8% error; and the signal to background ratio is 1:2 (again from [22]), with a systematic error on the background of 1.8%. Therefore, an experiment at the Tevatron in Run 3 will see approximately 1146 events when searching for W^*

single top quark production, with one-third signal events and two-thirds coming from various backgrounds (e.g., $W+b\bar{b}$, $W+$ light jets with two mistags, WZ with $Z\rightarrow b\bar{b}$, W -gluon fusion, and $t\bar{t}$). This observation will lead to a measurement of the W^* single top quark production cross section with an error of 7% (statistical) \oplus 6% (systematic) = 10% . Smith and Willenbrock [24] show that the error on the theoretical cross section for W^* single top quark production is only 3%, leading to an error on V_{tb} of 5%.

In Fig. 10 we show the results of these calculations, extended into the (V_{tb}, A_r) plane. In plot 10(a) for Tevatron Run 2 (2 fb^{-1}), the outer short-dashed contours show the result when the error on the theory cross section includes a 30% contribution from lack of knowledge of the gluon distribution. The inner long-dashed contours result from when this error contributes only 10% to the overall measurement. Plot 10(b) presents our estimates for Tevatron Run 3, ‘‘TeV33’’ (30 fb^{-1}), with the dashed contours showing the precision obtainable using a theory error of only 3% and an experimental search to isolate the W^* s -channel mode of single top quark production. We discuss in the next subsection how one might distinguish standard model production from the $(V+A)$ scenario discussed above where the effects of an elevated cross section caused by the anomalous coupling cancel with a reduced value of V_{tb} from a possible mixing of the top quark with a new fourth generation quark to give an observed number of events consistent with the standard model.

C. Polarization of the top quark

Top quark polarization depends strongly on the structure of the Wtb coupling, and one might expect an asymmetry in angular distributions of the final state partons for different values of A_r . For example, standard model single top quarks are produced almost 100% left-handedly polarized because of the left-handed current structure of the Wtb coupling, whereas if $A_r=1$, the top quarks are not polarized at all. To calculate polarization effects using Monte Carlo generators, it is necessary either to keep the polarization of all particles

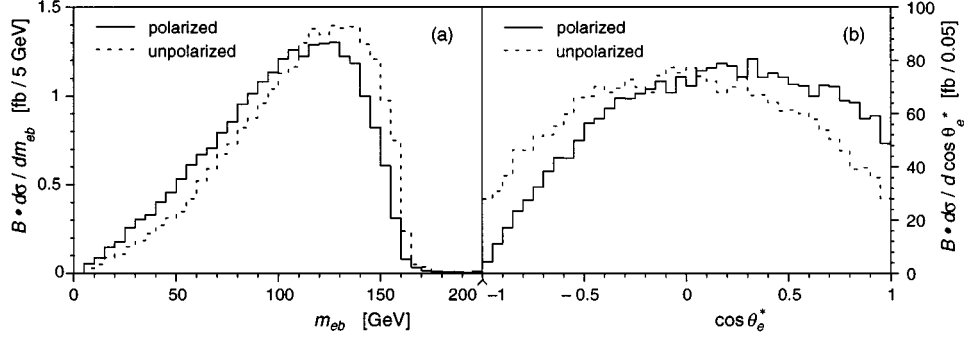


FIG. 11. Distributions of (a) invariant mass m_{eb} , and (b) cosine of the polar angle θ_e^* (defined in the text for single top quark production). The solid histograms are for the standard model case where the top quark and W boson are $\sim 100\%$ left-handedly polarized (fully calculated using CompHEP for the $2 \rightarrow 4$ and $2 \rightarrow 5$ processes with intermediate state t and W resonances), and the dashed histograms are for when there is no polarization, corresponding either to a $(V+A)$ term with $A_r=1$ in the Wtb coupling, or to the case where the polarization has been excluded from the calculation (e.g., by using PYTHIA to decay the W boson).

in the final states of the $2 \rightarrow 2$ and $2 \rightarrow 3$ processes being studied (i.e., $q' \bar{q} \rightarrow t \bar{b}$, $q' b \rightarrow tq$, $q' g \rightarrow tq \bar{b}$), with subsequent decays of the polarized top quark and W boson ($t \rightarrow Wb$, $W \rightarrow e\nu$), or else one needs to calculate the higher order $2 \rightarrow 4$ and $2 \rightarrow 5$ processes (i.e., $q' \bar{q} \rightarrow e\nu b \bar{b}$, $q' b \rightarrow e\nu bq$, $q' g \rightarrow e\nu bq \bar{b}$), with the top quark and W boson treated as resonances in the intermediate states. The second method automatically includes the polarizations of the intermediate state t and W . To study the differences between kinematic distributions when the polarizations of the top quark and W boson have been taken into account with those where they are assumed to be unpolarized (as in most Monte Carlo generators, e.g., PYTHIA), we have calculated the $2 \rightarrow 4$ and $2 \rightarrow 5$ processes for the three significant single top quark production modes using CompHEP alone, and compared the results with calculations where we used CompHEP for the $2 \rightarrow 2$ and $2 \rightarrow 3$ single top quark processes, and PYTHIA for the subsequent t and W decays.

Our direct calculations show that the p_T and η distributions are not sensitive to the polarization of the top quark.

Two representative examples of distributions expected to reflect the top quark polarization effects are the invariant mass of the positron and the b quark m_{eb} , and the cosine of the polar angle $\cos \theta_e^*$. The invariant mass m_{eb} is given by

$$m_{eb} = \sqrt{(E_e + E_b)^2 - (p_{Te} + p_{Tb})^2 - (p_{ze} + p_{zb})^2},$$

where p_z is the momentum of the positron or b quark along the beam direction.

The polar angle θ_e^* is defined as the angle between the positron direction and the x axis within the rest frame of the W boson, where the x axis is defined to be in the direction of motion of the W boson in the rest frame of the top quark [16]. The cosine of this angle is given approximately by

$$\cos \theta_e^* \approx 1 - \frac{2m_{eb}}{m_t^2 - m_W^2}.$$

Figure 11 shows the distributions of (a) m_{eb} and (b) $\cos \theta_e^*$, for the case when polarizations of the top quark and W boson have been properly taken into account (solid histogram), and for when summation over the polarization of the

top quark decay products has been done using the subsequent decays of an unpolarized top quark and W boson (dashed histogram). One can see that there are indeed differences in these distributions for the polarized and unpolarized cases. In particular, an asymmetry (or lack of it) in $\cos \theta_e^*$ when the positron is emitted aligned or antialigned with the direction of motion of the W boson in the top quark rest frame should be observable with high statistics. All three modes of single top quark production exhibit this same behavior. The two variables m_{eb} and $\cos \theta_e^*$ can also be used in combination with the total single top quark production rate, which is sensitive to the Wtb coupling structure as shown previously, to further our understanding of the Wtb coupling.

D. Top quark partial width

From our estimates of the sensitivity for measuring the single top quark cross section at future Tevatron runs, we can obtain an estimate of the expected precision on the top quark partial width $\Gamma(t \rightarrow WX)$, where X is any particle which can originate from the partons inside the proton or antiproton. In the standard model, X consists primarily of b quarks, with small contributions from s and d quarks. Because the top quark partial width is proportional to the t - and u -channel single top quark cross section divided by the flux for producing a W boson from the initial state (constant for a given energy \sqrt{s}) [19], the error on the top quark partial width is just the experimental measurement error on this cross section added in quadrature with the theoretical calculation error. For this estimate, we conservatively assume that all the W^* s -channel single top quark events become background and are not rejected in the analysis, and so the signal to background ratio changes from 1:2 to 1:3.2. Therefore, of the 650 events predicted to be observed in Run 2, approximately 153 will be from subprocesses 2.1 $q' b \rightarrow tq$ and W -gluon fusion 2.2 $q' g \rightarrow tq \bar{b}$. This gives an experimental error on the cross section of 15% (statistical) \oplus 24% (systematic) = 28%. The theoretical error is 32% (16%) as before, when the error on the gluon distribution function is assumed to be 30% (10%). Therefore, the error on the top quark partial width $\Gamma(t \rightarrow WX)$ from Run 2 data will be 28% \oplus 32% (16%) = 43% (32%). Extending this result from 2 fb^{-1} to 30 fb^{-1}

and using the better-measured gluon distribution function error of 10% leads to a prediction of the error on the top quark partial width of $[4\%(\text{stat}) \oplus 8\%(\text{syst})]_{\text{expt}} \oplus [13\%(\text{parton distribution and scale}) \oplus 10\%(\text{gluon distribution})]_{\text{theory}} = 19\%$. This is about one-half as good as that achievable at a linear e^+e^- collider [81] using a $t\bar{t}$ threshold scan, but the measurement can be made many years sooner, so will still be valuable.

IV. CONCLUSIONS

In this paper we have reported the results of new studies of single top quark physics at the Fermilab Tevatron $p\bar{p}$ collider. We have made consistent calculations of the tree level cross sections for each mode of single top quark production as a function of top quark mass, parton distribution function, QCD scale, and collision energy. We discussed details of the calculations for several of the subprocesses involved, and gave breakdowns of the various contributions to the overall cross sections. For a top quark of mass 180 GeV, at $\sqrt{s} = 1.8$ TeV, with $Q^2 = m_t^2$, and taking the mean result from CTEQ3M and MRS(A'), we find that the leading order total single top quark plus antiquark cross section is $1.76^{+0.26}_{-0.18}$ pb.

We have shown for each subprocess separately the transverse momentum and pseudorapidity distributions of the top quark, the other quarks produced with it, and its decay products. These kinematic distributions need to be understood in order to be able to separate signal from background in an experimental search.

We then considered the possibility for measuring the CKM matrix element V_{tb} and the Wtb coupling directly using single top quark events from the next Tevatron run. We estimated the sensitivity such measurements might have, and how an anomalous ($V+A$) term in the Wtb coupling would

affect the measurement of V_{tb} . If there is no anomalous component to the Wtb coupling, then V_{tb} can be measured to a precision of 19% or 12% in Run 2 (1999–2001), with the two values coming from different estimates of the uncertainty in the gluon distribution function. In Run 3 (2002–2006), the precision on V_{tb} will be improved to 5%. The top quark polarization affects the angular distributions of its decay products, and we investigated how this could be used together with a measurement of the single top quark cross section to distinguish between various processes affecting the top quark beyond the standard model. Finally, our estimates of the single top quark cross section error show that the top quark partial width $\Gamma(t \rightarrow WX)$ will be measured to within 43%–32% in Run 2, and to a precision of 19% in Run 3.

We find the prospects for single top quark physics at the Tevatron exciting and that a rich program of studies will be possible in future.

ACKNOWLEDGMENTS

We would like to thank Dan Amidei, Asher Klatchko, Wu-Ki Tung, Scott Willenbrock, C.-P. Yuan, and our colleagues in the DØ Collaboration for useful discussions during this work. We would also like to thank the Moscow State University CompHEP group, especially Slava Ilyin and Alexander Pukhov for their help with the latest version of CompHEP. We acknowledge the financial support of the U.S. Department of Energy under Grant No. DE-FG03-94ER40837, and the Ministry of Science and Technology Policy in Russia. This work was supported in part by Grant No. M9B000 from the International Science Foundation, in part by RFBR Grant Nos. 96-02-19773a and 96-02-18635a, and by Grant No. 95-0-6.4-38 of the Center for Natural Sciences of the State Committee for Higher Education in Russia.

-
- [1] DØ Collaboration, S. Abachi *et al.*, Phys. Rev. Lett. **74**, 2632 (1995).
 - [2] CDF Collaboration, F. Abe *et al.*, Phys. Rev. Lett. **74**, 2626 (1995).
 - [3] P. Grannis, plenary talk at the International Conference on High Energy Physics, Warsaw, 1996, reporting the analysis of the DØ and CDF Collaborations.
 - [4] A. Blondel, plenary talk at the International Conference on High Energy Physics, Warsaw, 1996, reporting the analysis of the LEP Electroweak Working Group and the SLD Heavy Flavor Group, CERN Internal Report No. LEPEWWG/96-02, available at <http://www.cern.ch/LEPEWWG>
 - [5] R. D. Peccei, S. Peris, and X. Zhang, Nucl. Phys. **B349**, 305 (1991).
 - [6] N. Cabibbo, Phys. Rev. Lett. **10**, 531 (1963); M. Kobayashi and T. Maskawa, Prog. Theor. Phys. **49**, 652 (1973).
 - [7] Particle Data Group, R. M. Barnett *et al.*, Phys. Rev. D **54**, 1 (1996).
 - [8] S. Dawson, Nucl. Phys. **B249**, 42 (1985).
 - [9] S. S. D. Willenbrock and D. A. Dicus, Phys. Rev. D **34**, 155 (1986).
 - [10] S. Dawson and S. S. D. Willenbrock, Nucl. Phys. **B284**, 449 (1987).
 - [11] C.-P. Yuan, Phys. Rev. D **41**, 42 (1990).
 - [12] T. Moers, R. Priem, D. Rein, and H. Reitler, in *Proceedings of the ECFA Large Hadron Collider (LHC) Workshop: Physics and Instrumentation*, Aachen, Germany, 1990, edited by G. Jarlskog and D. Rein (CERN, Geneva, 1990), Vol. 2, p. 418.
 - [13] G. V. Jikia and S. R. Slabospitsky, Phys. Lett. B **295**, 136 (1992).
 - [14] R. K. Ellis and S. Parke, Phys. Rev. D **46**, 3785 (1992).
 - [15] G. Bordes and B. van Eijk, Z. Phys. C **57**, 81 (1993).
 - [16] D. O. Carlson and C.-P. Yuan, Phys. Lett. B **306**, 386 (1993).
 - [17] G. Bordes and B. van Eijk, Nucl. Phys. **B435**, 23 (1995).
 - [18] D. O. Carlson and C.-P. Yuan, MSUHEP-40903, 1995 (unpublished).
 - [19] D. O. Carlson and C.-P. Yuan, in *Proceedings of the 17th International Warsaw-Kazimierz Meeting on Particle Physics, and Madison Phenomenology Symposium*, Ames, Iowa, 1995, edited by K. E. Lassila, J. Qiu, A. Sommerer, G. Valencia, K. Whisnant, and B. L. Young (World Scientific, Singapore, 1996), p. 172.

- [20] A. P. Heinson, A. S. Belyaev, and E. E. Boos, in *Proceedings of the 17th International Warsaw-Kazimierz Meeting on Particle Physics, and Madison Phenomenology Symposium* [19], p. 202.
- [21] S. Cortese and R. Petronzio, *Phys. Lett. B* **253**, 494 (1991).
- [22] T. Stelzer and S. Willenbrock, *Phys. Lett. B* **357**, 125 (1995).
- [23] R. Pittau, *Phys. Lett. B* **386**, 397 (1996).
- [24] M. Smith and S. Willenbrock, *Phys. Rev. D* **54**, 6696 (1996).
- [25] D. Atwood, S. Bar-Shalom, G. Eilam, and A. Soni, *Phys. Rev. D* **54**, 5412 (1996).
- [26] C. S. Li, R. J. Oakes, and J. M. Yang, *Phys. Rev. D* **55**, 1672 (1997).
- [27] C. S. Li, R. J. Oakes, and J. M. Yang, *Phys. Rev. D* **55**, 5780 (1997).
- [28] D. O. Carlson, E. Malkawi, and C.-P. Yuan, *Phys. Lett. B* **337**, 145 (1994).
- [29] E. Malkawi and C.-P. Yuan, *Phys. Rev. D* **50**, 4462 (1994).
- [30] C.-P. Yuan, *Mod. Phys. Lett. A* **10**, 627 (1995).
- [31] T. G. Rizzo, *Phys. Rev. D* **53**, 6218 (1996).
- [32] G. Mahlon and S. Parke, *Phys. Rev. D* **55**, 7249 (1997).
- [33] M. Katuya, J. Morishita, T. Munehisa, and Y. Shimizu, *Prog. Theor. Phys.* **75**, 92 (1986).
- [34] V. Barger and K. Hagiwara, *Phys. Rev. D* **37**, 3320 (1988).
- [35] M. Raidal and R. Vuopionperä, *Phys. Lett. B* **318**, 237 (1993).
- [36] O. Panella, G. Pancheri, and Y. N. Srivastara, *Phys. Lett. B* **318**, 214 (1993).
- [37] K. Hagiwara, M. Tanaka, and T. Stelzer, *Phys. Lett. B* **325**, 521 (1994).
- [38] S. Ambrosanio and B. Mele, *Z. Phys. C* **63**, 63 (1994).
- [39] E. Boos *et al.*, *Phys. Lett. B* **326**, 190 (1994).
- [40] N. V. Dokholian and G. V. Jikia, *Phys. Lett. B* **336**, 251 (1994).
- [41] E. Boos, Y. Kurihara, Y. Shimizu, M. Sachwitz, H. J. Schreiber, and S. Shichanin, *Z. Phys. C* **70**, 255 (1996).
- [42] M.-L. Qian, W.-G. Ma, L.-Z. Sun, and Y.-Y. Liu, *J. Phys. G* **20**, 895 (1994).
- [43] A. Ballestrero, V. A. Khoze, E. Maina, S. Moretti, and W. J. Stirling, *Z. Phys. C* **72**, 71 (1996).
- [44] G. V. Jikia, *Nucl. Phys.* **B374**, 83 (1992).
- [45] E. Yehudai, S. Godfrey, and K. A. Peterson, in *Proceedings of the Second International Workshop on Physics and Experiments with Linear e^+e^- Colliders*, Waikoloa, Hawaii, 1993, edited by F. A. Harris, S. L. Olsen, S. Pakvasa, and X. Tata (World Scientific, Singapore, 1993), Vol. 2, p. 568.
- [46] E. Boos, A. Pukhov, M. Sachwitz, and H. J. Schreiber, *Z. Phys. C* **75**, 237 (1997).
- [47] E. E. Boos *et al.*, in *Proceedings of the XXVth Rencontres de Moriond, High Energy Hadronic Interactions*, Les Arcs, France, 1991, edited by J. Tran Than Van (Editions Frontieres, Gif-sur-Yvette, 1991), p. 501; E. E. Boos *et al.*, in *Proceedings of the Second International Workshop on Software Engineering, Artificial Intelligence and Expert Systems for High Energy and Nuclear Physics*, La Londe Les Maures, France, 1992, edited by D. Perret-Gallix (World Scientific, Singapore, 1992), p. 665. COMPHEP is available at <http://theory.npi.msu.su/~pukhov/comphep.html>
- [48] S. Kawabata, *Comput. Phys. Commun.* **41**, 127 (1986).
- [49] V. A. Ilyin, D. N. Kovalenko, and A. E. Pukhov, Moscow State University, INP MSU Report No. 95-2/366, 1995.
- [50] G. P. Lepage, *J. Comput. Phys.* **27**, 192 (1978).
- [51] T. Sjöstrand, *Comput. Phys. Commun.* **82**, 74 (1994). PYTHIA version 5.7 was used.
- [52] CTEQ Collaboration, H. L. Lai *et al.*, *Phys. Rev. D* **51**, 4763 (1995).
- [53] A. D. Martin, R. G. Roberts, W. J. Stirling, *Phys. Lett. B* **354**, 155 (1995).
- [54] W. A. Bardeen, A. J. Buras, D. W. Duke, and T. Muta, *Phys. Rev. D* **18**, 3998 (1978).
- [55] CTEQ Collaboration, H. L. Lai *et al.*, *Phys. Rev. D* **55**, 1280 (1997).
- [56] A. D. Martin, R. G. Roberts, and W. J. Stirling, *Phys. Lett. B* **387**, 419 (1996).
- [57] V. N. Gribov and L. N. Lipatov, *Sov. J. Nucl. Phys.* **15**, 438 (1972); **15**, 675 (1972); Yu. L. Dokshitzer, *Sov. Phys. JETP* **46**, 641 (1977); G. Altarelli and G. Parisi, *Nucl. Phys.* **B126**, 298 (1977).
- [58] R. M. Barnett, H. E. Haber, and D. E. Soper, *Nucl. Phys.* **B306**, 697 (1988).
- [59] F. I. Olness and W.-K. Tung, *Nucl. Phys.* **B308**, 813 (1988).
- [60] W.-K. Tung (private communication).
- [61] E. L. Berger and H. Contopanagos, *Phys. Lett. B* **361**, 115 (1995); *Phys. Rev. D* **54**, 3085 (1996).
- [62] CTEQ Collaboration, J. Botts *et al.*, *Phys. Lett. B* **304**, 159 (1993).
- [63] U. Heintz *et al.*, in “Future Electroweak Physics at the Fermilab Tevatron – Report of the tev_2000 Study Group,” Fermilab, 1996, edited by D. Amidei and R. Brock, Report No. FERMILAB-PUB-96/082, 1996 (unpublished), p. 136.
- [64] G. Marchesini *et al.*, *Comput. Phys. Commun.* **67**, 465 (1992).
- [65] N. G. Deshpande, B. Margolis, and H. D. Trottier, *Phys. Rev. D* **45**, 178 (1992).
- [66] D. Atwood, A. Aepli, and A. Soni, *Phys. Rev. Lett.* **69**, 2754 (1992).
- [67] D. Atwood, A. Kagan, and T. G. Rizzo, *Phys. Rev. D* **52**, 6264 (1995).
- [68] C.-S. Huang and T.-J. Li, *Z. Phys. C* **68**, 319 (1995).
- [69] K. Cheung, *Phys. Rev. D* **53**, 3604 (1996).
- [70] J. Berger, A. Blotz, H.-C. Kim, and K. Goetze, *Phys. Rev. D* **54**, 3598 (1996).
- [71] T. Tait and C.-P. Yuan, *Phys. Rev. D* **55**, 7300 (1997).
- [72] C. T. Hill, *Phys. Lett. B* **266**, 419 (1991).
- [73] C. T. Hill and S. J. Parke, *Phys. Rev. D* **49**, 4454 (1994).
- [74] E. Eichten and K. Lane, *Phys. Lett. B* **327**, 129 (1994).
- [75] L. L. Smith, P. Jain, and D. W. McKay, in *Proceedings of the 9th Annual American Physical Society Division of Particles and Fields Meeting*, Minneapolis, MN, 1996 (unpublished), hep-ph/9608328.
- [76] A. Datta and X. Xiang, *Phys. Rev. D* **55**, 2530 (1997).
- [77] E. H. Simmons, *Phys. Rev. D* **55**, 5494 (1997).
- [78] D. Amidei *et al.*, in “Future Electroweak Physics at the Fermilab Tevatron – Report of the tev_2000 Study Group,” Fermilab, 1996 [63], p. 13.
- [79] C.-P. Yuan (private communication).
- [80] H. Weerts (private communication).
- [81] R. Frey, in *Proceedings of the 3rd Workshop on Physics and Experiments with e^+e^- Linear Colliders*, Iwate, Japan, 1995, edited by A. Miyamoto, Y. Fujii, T. Matsui, and S. Iwata (World Scientific, Singapore, 1996), p. 144.